PHYSICAL REVIEW B **86**, 241304(R) (2012)

Phonon-assisted incoherent excitation of a quantum dot and its emission properties

S. Weiler,* A. Ulhaq, S. M. Ulrich, D. Richter, M. Jetter, and P. Michler
Institut für Halbleiteroptik und Funktionelle Grenzflächen, Universität Stuttgart, Allmandring 3, 70569 Stuttgart, Germany

C. Roy and S. Hughes
Department of Physics, Engineering Physics and Astronomy, Queens's University, Kingston, Ontario K7L 3N6, Canada
(Received 7 March 2012; published 26 December 2012)

We present a detailed study of a phonon-assisted incoherent excitation mechanism of single quantum dots. A spectrally detuned continuous-wave laser couples to a quantum dot transition by mediation of acoustic phonons, whereby excitation efficiencies up to 20% with respect to strictly resonant excitation can be achieved at $T = 9$ K. Laser-frequency-dependent analysis of the quantum dot intensity distinctly maps the underlying acoustic phonon bath and shows good agreement with our polaron master equation theory. An analytical solution for the steady-state exciton density (which is proportional to the photoluminescence) is introduced which predicts a broadband incoherent coupling process mediated by electron-phonon scattering. Moreover, we investigate the coherence properties of the emitted light with respect to strictly resonant versus phonon-assisted excitation, revealing the importance of narrow band triggered emitter-state initialization for possible applications of a quantum dot exciton system as a qubit.

DOI: 10.1103/PhysRevB.86.241304 PACS number(s): 78.67.Hc, 63.20.kk, 78.55.−m

Important properties of nonclassical light emission from a single quantum dot (QD), e.g., its exciton linewidth and coherence properties, depend on the physical nature of the excitation process of the QD. A standard method to address QDs optically is through excitation into the barrier or wetting layer, which causes subsequent capture and relaxation, finally resulting in the recombination of carriers and the emission of photons. Such an *incoherent pumping* mechanism leads to homogeneous broadening of the excited state and results in a reduction in coherence time. A more selective excitation of a single QD is possible via pumping into a higher electronic (*d* or *p* shell) or the QD ground state (*s* shell). The latter technique is suitable for generation of photons that are close to Fourier transform limited.[1]

Due to the distinct coupling of QD confined-state dynamics to the surrounding solid-state crystal, phonon-mediated excitation offers an alternative means of selective emitter state preparation. For instance, pumping of single QDs via an energetically sharp longitudinal-optical (LO) phonon resonance, ∼35 meV above the dot ground state, has been demonstrated.[2–5] Besides LO phonon coupling, other optical excitation methods rely on the interaction of the electron-hole pair with acoustic phonons, for instance, nonresonant coupling (NRC) between emitter and cavity.[6–8] This effect causes a detuned cavity mode to be efficiently excited by a QD coupled to the surrounding acoustic phonon bath. The inverse nonresonant coupling effect, where the QD is excited via cavity photon emission, has also been demonstrated experimentally.[9] Recent theoretical analysis in the context of the nonresonant coupling effect, however, has shown that simple Lorentzian-like pure dephasing models are not sufficient to fully explain this phenomenon.[6,7,10] Especially in the domain of resonance fluorescence, where the QD-cavity system is excited coherently, significant phonon-induced coupling between the QD exciton and the cavity is predicted,[11] resulting in phonon-mediated excitation-induced dephasing (EID) and pronounced exciton-cavity feeding. The former EID mechanism has been observed in micropillar-QD systems,[12] and related EID phenomena have been measured using coherently excited QDs with pulsed lasers.[13] Excitation-induced dephasing, via resonance fluorescence, manifests in spectral broadening of the Mollow triplet sidebands as the strength of the pump field is increased; however, it does not give any direct information about the spectral characteristics of the broad phonon bath. The exciton-acoustic phonon coupling is also directly observable via the broad phonon bands on the higher and lower energetic sides of the zero-phonon line (ZPL), which can be theoretically explained by the independent boson model[14] with consideration of pure dephasing effects.[15,16] The ZPL is Fourier limited up to a first approximation but higher order coupling terms lead to a broadening,[17] which increases with temperature. These phonon-based pure dephasing effects have been experimentally studied in detail, particularly using the highly phase-sensitive technique of four-wave mixing.[18] The longitudinal acoustic (LA) phonon sidebands have also been directly observed in QD emission spectra at elevated temperatures,[19,20] using incoherent excitation (i.e., pump laser excitation that is spectrally far detuned from the target exciton state).

In this article, we present a joint experimental-theory investigation of phonon-mediated incoherent excitation in the polaron regime. The clear signature of phonon-mediated excitation is quite distinct from all previous attempts at exploring electron-phonon interactions in QDs, and we present an unequivocal and more direct probe of the phonon bath. We introduce a transparent analytical model for the excited QD–phonon-bath system in a planar sample such that the coupling between laser photons and a QD is mediated by acoustic phonons in the framework of an effective phonon master equation (ME),[21] which is derived from a full polaron ME.[11] We show that the effective QD intensity is a direct result of phonon-mediated coupling, which depends on the phonon density of states at the laser excitation energy and the pump intensity of the field. Moreover, this results in an incoherent excitation process that is a direct signature of exciton-phonon

coupling effects beyond a weak exciton-phonon coupling approach—where such a mechanism is either missing in a pure dephasing only model[22] or hard to interpret.[23] Inspired by related theoretical predictions that show that the phonon local density of states can be mapped via detuned resonance fluorescence,[21,24] we experimentally demonstrate the effective pumping of a single QD via LA phonon coupling by spectrally tuning the continuous-wave laser close to the QD s-shell resonance within the range of LA phonon energies. The detuning-dependent frequency scans yield QD intensity profiles exhibiting both the ZPL profile and the broad LA phonon sidebands (spanning more than 5 meV). Additionally, we measure the coherence time of QD emission excited via this incoherent excitation process in comparison to that for strictly resonant cw excitation. We also discuss these findings in the perspective of optimized qubit initialization, particularly for the application-oriented conditions of triggered exciton-state excitation.

For our experiments, we employed self-assembled In(Ga,As)/GaAs QDs grown by metal-organic vapor-phase epitaxy. A single layer of QDs was centered in a 1-λ-thick planar GaAs cavity surrounded by alternating $\lambda/4$ periods of AlAs/GaAs as 4 top and 20 bottom distributed Bragg reflectors. The sample was mounted in a He-flow cryostat at controllable temperatures of $T = 4$–15 K. For resonant laser stray-light suppression an orthogonal excitation-detection geometry microphotoluminescence (μPL) setup in combination with a pinhole assembly and polarizer was used. The sample was excited by a narrow band (~500 kHz) tunable Ti:Sapphire continuous wave laser. More details of the experimental techniques and the setup are given in Refs. 1, 25, and 26.

Figure 1 illustrates the effect of phonon-assisted incoherent excitation of a QD. For the experimental conditions shown, the laser excitation is energetically blue-detuned from the emitter by $\Delta = (\omega_L - \omega_{QD}) = 596$ μeV. Even though the laser is not resonant with any higher QD shells (energetic

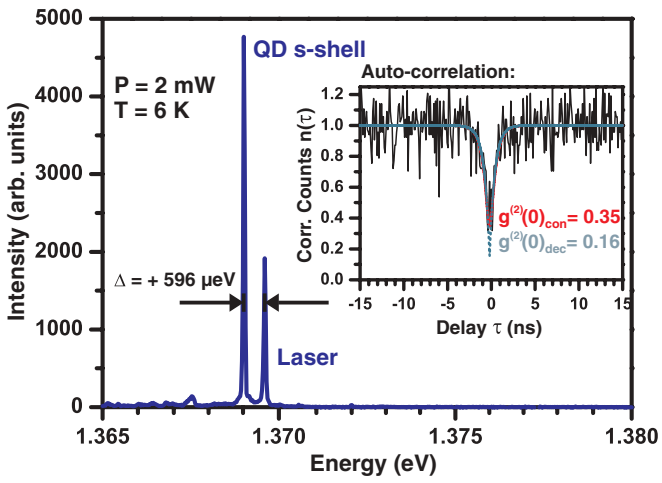

FIG. 1. (Color online) Demonstration of phonon-assisted incoherent excitation of a single QD. PL emission sprectrum of a QD nonresonantly excited via a cw laser ($\Delta = 596$ meV). Inset: Corresponding autocorrelation measurement on the QD s shell proving almost-background-free single-photon emission with a deconvoluted antibunching value (detector response) of $g^{(2)}(0)_{dec} = 0.16 \pm 0.02$ [convoluted: $g^{(2)}(0)_{con} = 0.35 \pm 0.04$].

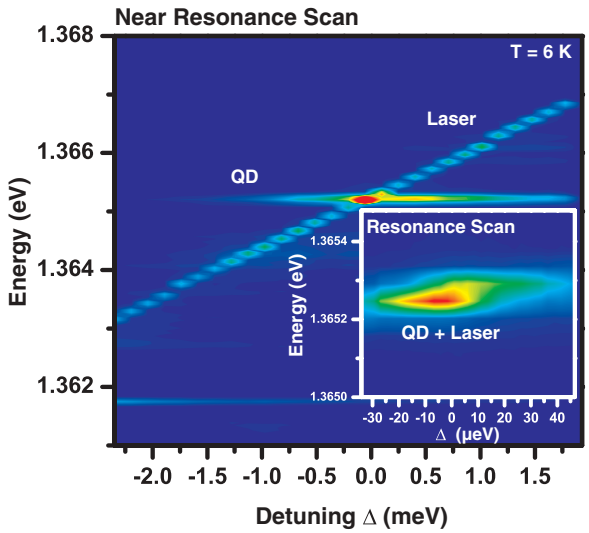

FIG. 2. (Color online) Near-resonance frequency scan: The excitation laser energy was systematically varied in steps of ~15 μeV to scan over the QD s shell at a fixed power of $P = 500$ μW. As is evident from the color plot, emission from the QD can be continuously traced. Inset: Resonance scan. Detailed scan over the QD s shell in steps of ~2 μeV revealing the onset of resonance fluorescence around $\Delta = 0$.

separation between s- and p-shell separation is typically ~25 meV), considerable emitter intensity can be observed in the μPL spectrum. The inset in Fig. 1 shows the corresponding autocorrelation measurement of QD photons unambiguously proving the single-photon emission nature with a $g^{(2)}(0)$ value of 0.16 ± 0.02, deconvoluted with respect to the setup time resolution of 450 ps [convoluted value: $g^{(2)}(0) = 0.35 \pm 0.04$].

To gain more insight into the effect of the phonon-induced incoherent excitation, we scanned the cw laser over the QD resonance in steps of ~15 μeV. Under constant excitation power, a μPL spectrum is taken at each step ($P = 500$ μW, $T = 5$ K). The PL data depicted in Fig. 2 reveal appreciable QD emission over a long range of frequencies even away from the s-shell resonance. The persistent presence of the QD signal for a relatively large range of laser energies rules out excitation of the QD via the quantized energy eigenstates of the dot itself. Instead we attribute the excitation of the QD over a continuum of frequencies to the presence of the LA phonon bath. The QD is effectively excited by either emitting ($\Delta > 0$) or absorbing ($\Delta < 0$) phonons which compensate for the energy difference between the excitation source and the exciton s-shell energy. The inset in Fig. 2 (which shows a zoom into the region $\Delta \approx 0$) displays the fine frequency scan over the QD s shell with a step size of ~2 μeV. The increase in the signal towards $\Delta = 0$ reflects the clear onset of resonance fluorescence which overtakes the laser stray-light intensity in the composite fluorescence and laser signal. Remarkably, such a pronounced phonon-coupling effect occurs even without any cavity coupling.

The effect of phonon-induced excitation is modeled using a polaronic ME where explicit phonon-mediated processes have been considered and derived in the form of Liouvillian superoperators. A polaron ME has also been used to investigate QD Rabi oscillations.[27] The effective phonon model is explained

in detail in Ref. 21, which also includes a cavity system. For the current system of interest (i.e., with no cavity coupling), the ME is[21]

$$\frac{\partial\rho}{\partial t} = \frac{1}{i\hbar}[H_S', \rho(t)] + \frac{\gamma}{2}\mathcal{L}[\sigma^-] + \frac{\gamma'}{2}\mathcal{L}[\sigma_{11}] + \frac{\Gamma_{\rm ph}^{\sigma^+}}{2}\mathcal{L}[\sigma^+] + \frac{\Gamma_{\rm ph}^{\sigma^-}}{2}\mathcal{L}[\sigma^-], \quad (1)$$

with a polaron-transformed system Hamiltonian, $H_S' = \hbar(-\Delta - \Delta_P)\sigma^+\sigma^- + \hbar\eta_x\langle B\rangle(\sigma^- + \sigma^+)$, where $\langle B\rangle = \exp[-\frac{1}{2}\int_0^\infty d\omega \frac{J(\omega)}{\omega^2}\coth(\beta\hbar\omega/2)]$ is the thermally averaged bath displacement operator and $J(w) = \alpha_p\,\omega^3\exp(-\frac{\omega^2}{2\omega_b^2})$ is the characteristic phonon spectral function; $\eta_x = 2\Omega$ is the coherent pump rate of the QD exciton, $\sigma_{11} = \sigma^+\sigma^-$, with σ^+,σ^- the Pauli operators, and we incorporate the polaron shift (Δ_P) into the definition of $\omega_{\rm QD}$ (and thus Δ) below. The Lindblad operators, $\mathcal{L}[O] = 2O\rho O^\dagger - O^\dagger O\rho - \rho O^\dagger O$, describe dissipation through ZPL radiative decay and ZPL pure dephasing (γ'), as well as pump-driven incoherent scattering processes mediated by the phonon bath: $\Gamma_{\rm ph}^{\sigma^+/\sigma^-} = 2\langle B\rangle^2\eta_x^2\,{\rm Re}[\int_0^\infty d\tau e^{\pm i\Delta\tau}(e^{\phi(\tau)} - 1)]$, where $\phi(\tau) = \int_0^\infty d\omega\frac{J(\omega)}{\omega^2}[\coth(\hbar\omega/2k_bT)\cos(\omega\tau) - i\sin(\omega\tau)]$. Physically, the $\Gamma_{\rm ph}^{\sigma^-}$ process corresponds to an enhanced radiative decay, while the $\Gamma_{\rm ph}^{\sigma^+}$ process represents an incoherent excitation process. If the laser pump is within the vicinity of the phonon bath, then the QD exciton can be excited through phonon emission or absorption.[21] As well as having analytical phonon scattering rates in the polaronic regime, we can also use Eq. (1) to derive an explicit expression for the steady-state exciton population,

$$\bar{N}_x = \frac{1}{2}\left[1 + \frac{\Gamma_{\rm ph}^{\sigma^+} - \Gamma_{\rm ph}^{\sigma^-} - \gamma}{\Gamma_{\rm ph}^{\sigma^+} + \Gamma_{\rm ph}^{\sigma^-} + \gamma + \frac{4\eta_x^2\langle B\rangle^2\Gamma_{\rm pol}}{\Gamma_{\rm pol}^2 + \Delta^2}}\right], \quad (2)$$

where $\Gamma_{\rm pol} = \frac{1}{2}(\Gamma_{\rm ph}^{\sigma^+} + \Gamma_{\rm ph}^{\sigma^-} + \gamma + \gamma')$. For the planar system of interest, the QD intensity from the vertical decay channel of the sample is simply $I_{\rm QD} \propto \bar{N}_x$. Importantly, Eq. (2) includes the detuning and pump dependence of the phonon-induced scattering rates. We stress again that the incoherent excitation process described through $\mathcal{L}[\sigma^+]$ (see inset in Fig. 4 for a schematic of this process) does not appear in ME approaches that assume weak exciton-phonon coupling in the limit of pure dephasing only. Thus, our PL line shapes (measured and predicted) show clear evidence of phonon-bath-mediated incoherent excitation.

To compare with the theoretical predictions of Eq. (2), the experimentally derived near-resonance μPL scans have been evaluated in terms of normalized QD intensity versus detuning. The results of a scan as shown in Fig. 2 are displayed in Figs. 3(a) and 3(b) [filled (black) circles] revealing strong resonance fluorescence of the QD near $\Delta \approx 0$ and a less intense, but distinctly broad QD emission with a corresponding detuning range between $\Delta \approx -1.5$ meV and $\Delta \approx +2$ meV. The above-presented theoretical model has been fitted to the experimental data [solid (red) lines in Figs. 3(a) and 3(b)]. The depicted profiles consists of two parts, i.e., a rather *sharp* ZPL (Lorentzian profile) at the QD resonance and a broader phonon-assisted excitation feature around the ZPL. In the latter case, a distinct asymmetry for $\Delta > 0$ is clearly visible. This is a direct and unambiguous signature of the unequal probabilities for LA phonon absorption and emission at low temperatures. This incoherent scattering process is quite different from the incoherent feeding that would result from a fast interlevel decay process. To help identify this process further, we also plot the calculation when the $\Gamma_{\rm ph}^{\sigma^+}$ process is turned off, which confirms that the laser-driven incoherent excitation process is the dominant phonon scattering process.

For modeling the measurement data, the corresponding values for temperature T, pump rate η_x, and radiative decay γ have been experimentally derived by independent measurements and are therefore fairly accurate values within their experimental error. As shown in the inset in Fig. 3(a), η_x can be extracted from the HRPL data. For the conditions in Fig. 3(a) the center-to-sideband Rabi-splitting Ω is found to be $16.7 \pm 0.7\mu$eV (=4.04 ± 0.17 GHz), giving $\eta_x = \frac{2\Omega}{2\pi} = 5.32 \pm 0.23$ μeV. The radiative lifetimes for most of the QDs in the sample are found to be rather similar due to the absence of preferential radiative enhancement of selective QDs by Purcell-like effects. Independent time-correlated photon counting measurements have revealed a typical radiative decay time of 750–850 ps, which gives $\gamma \approx 0.77$–0.88 μeV. The coupling constant describing the interaction between the exciton and the LA phonons via deformation potential α_p, the pure dephasing rate γ', and the cutoff frequency ω_b (proportional to the inverse of the typical electronic localization length in the QD)[23] are then derived via fitting. It should be mentioned that in most of our measurements we observed somewhat higher QD intensities than theoretically expected for intermediate positive detunings [as shown in Fig. 3(a) around $\Delta = 2$ meV and Fig. 3(b) around $\Delta = 1.7$ meV]. This effect might be attributed to some additional dephasing apart from the LA phonon coupling, which could be caused by a variety of possible effects like phonon scattering from defects or trapped charges in the vicinity of the QD.[20] It may also be caused by a deviation from the simple bulklike spectral function that we have used for $J(\omega)$, though overall the qualitative fit is seen to be very good. Excitation via phonon coupling is observed to be rather efficient and approximately 20 % of the QD intensity is achieved with respect to strictly resonant excitation, with the distinct advantage that the laser stray light can be easily separated from the QD emission; this efficient phonon-induced excitation is unique to the QD environment and is substantially different from excitation of an atomic resonance.

To gain further insight into the effect of phonon-assisted incoherent excitation, we have systematically studied theoretically the effects of ω_b, T, α_p, and η_x on the resulting intensity profiles in Figs. 3(c), 3(d), 3(e), and 3(f), respectively. An increase in the cutoff frequency ω_b (i.e., a decrease in QD size) leads to a blue shift of the phonon reservoir replica of the QD intensity profile. In contrast, an increasing temperature T, pump rate η_x, or coupling factor α_p overall increases the QD intensity for off-resonant excitation conditions. This can also be seen in Figs. 3(a) and 3(b), where an increased temperature and pump rate lead to a higher emission efficiency in Fig. 3(b) compared to Fig. 3(a). For increasing temperature,

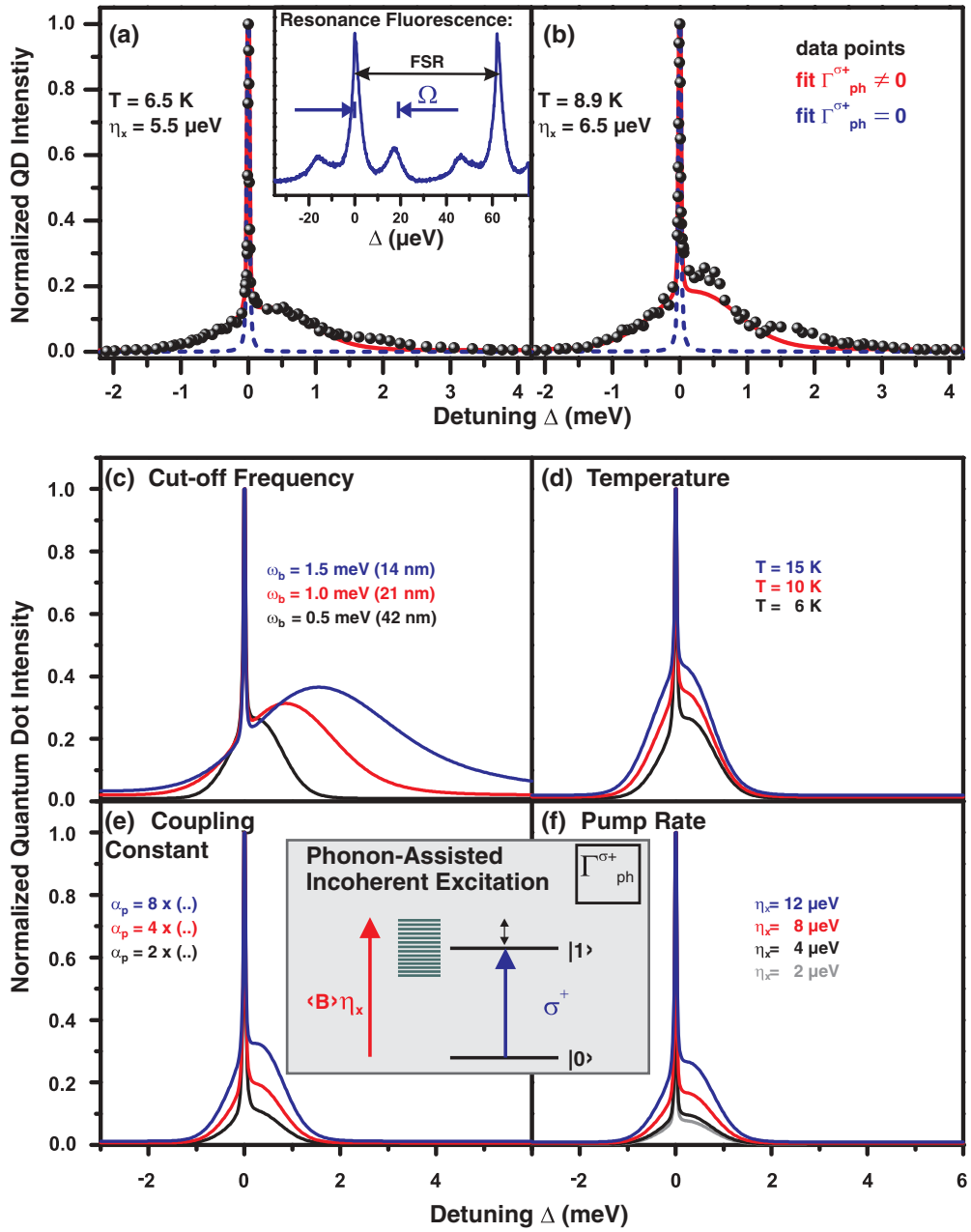

FIG. 3. (Color online) (a), (b) Intensity profiles: Integrated QD intensity derived from a frequency scan (similar to that in Fig. 2) plotted as a function of laser-QD detuning. The scans were performed at different temperatures. Experimental data indicated by (black) filled circles, and theory by solid (red) lines. The corresponding values used to fit the data with our theory [with phonon-induced processes $\Gamma^{\sigma^+}_{\rm ph}$ and $\Gamma^{\sigma^-}_{\rm ph}$, solid (red) line; with only the process $\Gamma^{\sigma^-}_{\rm ph}$, dashed (blue) line] are the cutoff frequency $\omega_b = 0.6$ meV, coupling parameter $\alpha_p = 6 \times 0.06 \times \pi^2$ ps^2, rate of radiative decay rate $\gamma = 0.82$ μeV (803 ps), and pure dephasing rate $\gamma' = 0.6$ μeV (1097 ps). The thermally averaged bath displacement operator is calculated to be $\langle B \rangle = 0.91$ for the conditions in (a) and $\langle B \rangle = 0.87$ for (b). Inset: HRPL spectrum with the characteristic resonance fluorescence spectrum in the frequency domain, revealing a Rabi energy (center to sideband) of $\Omega = 16.7 \pm 0.7$ μeV. (c)–(f) Investigation of the influence of the relevant parameters on the intensity profile of the QD emission. While keeping the other parameters fixed [$\omega_b = 0.5$ meV, $T = 6$ K, $\gamma = 0.8$ μeV (823 ps), $\gamma' = 0.8$ μeV, $\eta_x = 12$ μeV], the (a) phonon bath cutoff frequency ω_b, (b) temperature T, (c) coupling factor α_p, and (d) pump rate $\eta_x = 2\,\Omega$ were systematically increased from bottom to top respectively. Inset: The incoherent excitation process [left-hand (red) arrow], $\Gamma^{\sigma^+}_{\rm ph}$ scattering, mediated by the acoustic phonon bath [horizontally striped (green) rectangle].

these features become more symmetric due to increasing phonon-state occupations. Parameters α_p and η_x have similar effects on the shape of the intensity profile but keep the asymmetry unchanged. Variation of γ, γ' (not shown) mainly affects the width of the ZPL and has an almost-negligible effect on the broader intensity profile. We would like to emphasize that this effect has been observed consistently for several QDs in the sample.

Photon-visibility measurements have been performed by Michelson interferometry to determine the coherence

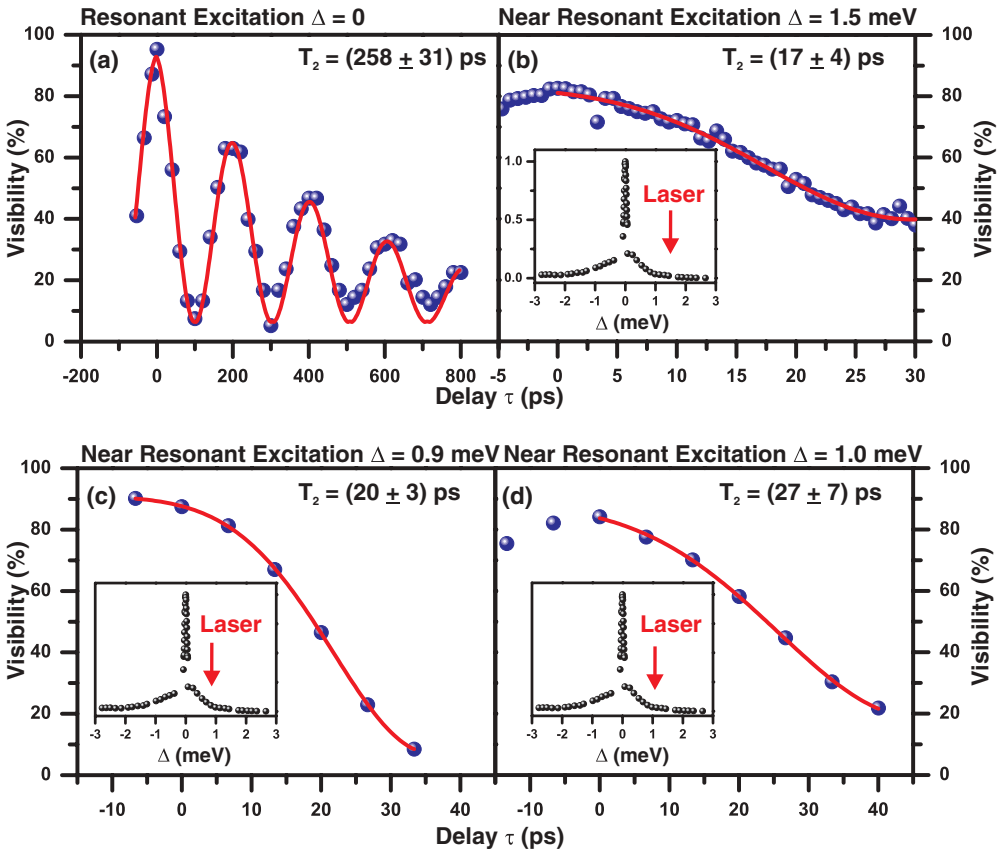

FIG. 4. (Color online) (a) Visibility measurements under strictly resonant and off-resonant (b)–(d) phonon-assisted incoherent excitation conditions. The off-resonant emission reveals the distinctly shorter T_2 of 17 ± 4 ps for $\Delta = 1.5$ meV, 20 ± 3 ps for $\Delta = 0.9$ meV, and 27 ± 7 ps for $\Delta = 1.0$ meV, in comparison to the resonant coherence of 258 ± 31 ps attributed to the phonon emission dephasing process. Solid lines are the corresponding Gaussian fits to the experimental data.

properties of photons emitted by both resonant and off-resonant excitation conditions. Figure 4(a) shows the sinusoidally varying visibility of the QD emission under strictly resonant excitation, which indicates the presence of a Mollow triplet[28,29] in the spectral regime. The data have been fitted by the function $g^{(1)}(\tau) = \frac{1}{2}e^{-\Gamma_{\text{pol}}\tau}e^{i\omega\tau} + \frac{1}{4}e^{-(\Gamma_{\text{tot}}/2)\tau}e^{i(\omega-\Omega)\tau} + \frac{1}{4}e^{-(\Gamma_{\text{tot}}/2)\tau}e^{i(\omega+\Omega)\tau}$, with $\Gamma_{\text{tot}} = \Gamma_{\text{pol}} + \Gamma_{\text{pop}}$ and $\Gamma_{\text{pop}} = \gamma + \Gamma_{\text{ph}}^{\sigma^+} + \Gamma_{\text{ph}}^{\sigma^-}$, where the exponential decay reflects the limited coherence, yielding $T_2 = 258 \pm 31$ ps. Even under strictly resonant excitation the coherence is not lifetime limited, which may be attributed to spectral diffusion effects. As a comparison, we experimentally investigated the emission coherence under the nonresonant excitation conditions of phonon-assisted excitation for different detunings Δ. The Gaussian fitting functions applied to the measurement results shown in Figs. 4(b)–4(d) reveal coherence times of $T_2 \sim 20$ ps, rather limited compared to the value under a resonant pump due to dephasing induced by the excitation mechanism.

For possible applications of QD excitons as qubits, our coherence time investigations are of significant importance for a careful triggered initialization of the emitter state. A pulsed and therefore spectrally broad laser (compared to narrow-band cw excitation) would have distinct overlap not only with the ZPL, but also with the acoustic phonon side wings. Under these conditions part of the electron hole creation in the QD would unavoidably occur via phonon-assisted incoherent excitation and drastically limit the usability of excitons as qubits. In order to minimize the contributions of incoherently excited excitons under triggered resonant emitter-state preparation, sophisticated pulse shaping techniques are required[30] to generate spectrally small pulses which reduce the acoustic phonon bath overlap. Due to the Fourier limitation these pulses are broader in time. A trade-off between narrow-band coherent excitation and a short enough pulse duration, below the lifetime of the exciton, has to be found to circumvent double-exciton excitation within one laser pulse and therefore assure the utilization of a QD as a possible qubit.

In conclusion, we have presented a detailed study of the phonon-assisted incoherent excitation effect for self-assembled QDs. The experimentally investigated dot intensity as a function of laser-QD detuning is in very good agreement with the polaronic ME model. Additionally, we have studied the coherence properties of QD emission via phonon-mediated excitation and the influence of different realistic parameters on the spectral shape of the intensity profile has been theoretically investigated, using a newly presented and simple analytical solution for the steady-state exciton population. Phonon-assisted incoherent excitation therefore provides not only a unique excitation mechanism of a semiconductor QD but also an effective new tool to map the characteristic features of the phonon bath present in such a solid-state quantum-emitter system.

We thank W.-M. Schulz for expert sample preparation. S. Weiler acknowledges financial support from the Carl-Zeiss-Stiftung. A. Ulhaq acknowledges funding from the International Max Planck Research School IMPRS-AM. This work was supported by the National Sciences and Engineering Research Council of Canada.

*Corresponding author: s.weiler@ihfg.uni-stuttgart.de

[1] S. Ates, S. M. Ulrich, S. Reitzenstein, A. Löffler, A. Forchel, and P. Michler, Phys. Rev. Lett. **103**, 167402 (2009).

[2] A. Lemaître, A. D. Ashmore, J. J. Finley, D. J. Mowbray, M. S. Skolnick, M. Hopkinson, and T. F. Krauss, Phys. Rev. B **63**, 161309(R) (2001).

[3] Y. Toda, O. Moriwaki, M. Nishioka, and Y. Arakawa, Phys. Rev. Lett. **82**, 4114 (1999).

[4] F. Findeis, A. Zrenner, G. Böhm, and G. Abstreiter, Phys. Rev. B **61**, 10579(R) (2000).

[5] R. Oulton, J. J. Finley, A. I. Tartakovskii, D. J. Mowbray, M. S. Skolnick, M. Hopkinson, A. Vasanelli, R. Ferreira, and G. Bastard, Phys. Rev. B **68**, 235301 (2003).

[6] S. Hughes, P. Yao, F. Milde, A. Knorr, D. Dalacu, K. Mnaymneh, V. Sazonova, P. J. Poole, G. C. Aers, J. Lapointe, R. Cheriton, and R. L. Williams, Phys. Rev. B **83**, 165313 (2011).

[7] M. Calic, P. Gallo, M. Felici, K. A. Atlasov, B. Dwir, A. Rudra, G. Biasiol, L. Sorba, G. Tarel, V. Savona, and E. Kapon, Phys. Rev. Lett. **106**, 227402 (2011).

[8] A. Majumdar, E. D. Kim, Y. Gong, M. Bajcsy, and J. Vučković, Phys. Rev. B **84**, 085309 (2011).

[9] M. Kaniber, A. Neumann, A. Laucht, M. F. Huck, M. Bichler, M.-C. Amann, and J. J. Finley, New J. Phys. **11**, 013031 (2009).

[10] U. Hohenester, Phys. Rev. B **81**, 155303 (2010).

[11] C. Roy and S. Hughes, Phys. Rev. Lett. **106**, 247403 (2011).

[12] S. M. Ulrich, S. Ates, S. Reitzenstein, A. Löffler, A. Forchel, and P. Michler, Phys. Rev. Lett. **106**, 247402 (2011).

[13] A. J. Ramsay, A. V. Gopal, E. M. Gauger, A. Nazir, B. W. Lovett, A. M. Fox, and M. S. Skolnick, Phys. Rev. Lett. **104**, 017402 (2010).

[14] G. D. Mahan, *Many Particle Physics* (Springer, Berlin, 2000).

[15] T. Takagahara, Phys. Rev. B **60**, 2638 (1999).

[16] B. Krummheuer, V. M. Axt, and T. Kuhn, Phys. Rev. B **65**, 195313 (2002).

[17] E. A. Muljarov and R. Zimmermann, Phys. Rev. Lett. **93**, 237401 (2004).

[18] P. Borri, W. Langbein, U. Woggon, V. Stavarache, D. Reuter, and A. D. Wieck, Phys. Rev. B **71**, 115328 (2005).

[19] L. Besombes, K. Kheng, L. Marsal, and H. Mariette, Phys. Rev. B **63**, 155307 (2001).

[20] I. Favero, G. Cassabois , R. Ferreira, D. Darson, C. Voisin, J. Tignon, C. Delalande, G. Bastard, Ph. Roussignol, and J. M. Gérard, Phys. Rev. B **68**, 233301 (2003).

[21] C. Roy and S. Hughes, Phys. Rev. X **1**, 021009 (2011).

[22] A. Moelbjerg, P. Kaer, M. Lorke, and J. Mørk, Phys. Rev. Lett. **108**, 017401 (2012).

[23] A. Nazir, Phys. Rev. B **78**, 153309 (2008).

[24] K. J. Ahn, J. Förstner, and A. Knorr, Phys. Rev. B **71**, 153309 (2005).

[25] S. Ates, S. M. Ulrich, A. Ulhaq, S. Reitzenstein, A. Löffler, S. Höfling, A. Forchel, and P. Michler, Nature Photon. **3**, 724 (2009).

[26] A. Ulhaq, S. Ates, S. Weiler, S. M. Ulrich, S. Reitzenstein, A. Löffler, S. Höfling, L. Worschech, A. Forchel, and P. Michler, Phys. Rev. B **82**, 045307 (2010).

[27] D. P. S. McCutcheon and A. Nazir, New J. Phys. **12**, 113042 (2010).

[28] B. R. Mollow, Phys. Rev. **188**, 1969 (1969).

[29] A. Muller, E. B. Flagg, P. Bianucci, X. Y. Wang, D. G. Deppe, W. Ma, J. Zhang, G. J. Salamo, M. Xiao, and C. K. Shih, Phys. Rev. Lett. **99**, 187402 (2007).

[30] A. Reinhad, T. Volz, M. Winger, A. Badolato, K. Hennessy, E. L. Hu, and A. Imamoglu, Nature Photon. **6**, 93 (2012).